AN EXPERIMENTAL STUDY OF A MAGNETICALLY EXCITED SELF-ACTING GAS LUBRICATED THRUST BEARING

by

Rolf E. Weingardt

S.M. Thesis Course II January, 1964

AN EXPERIMENTAL STUDY OF A MAGNETICALLY EXCITED SELF-ACTING GAS LUBRICATED THRUST BEARING

by

Rolf E. Weingardt
A.B., Columbia College, 1960
S.B., Columbia School of Engineering, 1961

Submitted in partial fulfillment
of the requirements for the
degree of master of
science

at the

Massachusetts Institute of Technology
January 1964

AN EXPERIMENTAL STUDY OF A MAGNETICALLY EXCITED SELF-ACTING GAS LUBRICATED THRUST BEARING

by

Rolf E. Weingardt

Submitted to the Department of Mechanical Engineering on September 30, 1963 in partial fulfillment of the requirements for the degree of Master of Science.

ABSTRACT

A magnetically-excited, self-acting, gas (ambient air) lubricated thrust bearing is experimentally investigated. The thrust bearing consists of two thrust plates. One of the plates is held perpendicular to the axis of rotation, while the other is given a precessional wobble about this same axis. The wobble of the one element causes ambient air to circulate between the two plates. A certain amount of load carrying capacity is developed by this circulating film of air. The load carrying capacity is investigated under no-rotation conditions for various geometrical film configurations. In addition to load capacity the torque exerted by the bearing, due to the circulation of the air film, is studied. Variation of the mean film thickness due to an impulsive and a step change in the load is observed to determine the dynamic behavior of the bearing.

Thesis Supervisor: H. H. Richardson

Title: Associate Professor of Mechanical Engineering.

ACKNOWLEDGEMENTS

The author would like to thank the members of the M.I.T. staff and faculty, especially Professor H. Richardson, for their assistance in the experimental work and preparations of this thesis. A special thanks goes to the author's father, who helped in the construction of the test apparatus.

The U.S. Navy was responsible for the presence of the author at M.I.T.

This thesis was supported in part by the U.S. Air Force under Contract AF 33(616)-7535 and sponsored by the Division of Sponsored Research of M.I.T.

TABLE OF CONTENTS

APPENDIX

LIST OF TABLES AND FIGURES

I. INTRODUCTION

All of the present practical types of self-acting, or non-pressurized, gas lubricated thrust bearings require that there be relative motion between a rotating plate known as the slider and the bearing itself. The purpose of this thesis is to determine whether a load carrying capacity can be developed and maintained in a bearing, by causing an air film to circulate between two parallel, non-rotating plates. By wobbling one of the plates with an amplitude of the same order as the desired film thickness, the desired circulation can be maintained.

The original concept for this bearing study arose from a paper by Amir Mahavandi and Fletcher Osterle[1*], in which the authors investigated a bearing with the slider in steady spin and precession. By numerically solving Reynold's equation for a compressible lubricant, they were able to determine the resulting pressure distribution. The authors then integrated the pressure distribution to obtain a value for the load capacity which they applied to a bevel bearing, in which the slider was beveled with respect to the bearing.

The results of the experimental study of the non-rotating, wobble bearing are compared with the theoretical results of Mahavandi and Osterle. In the experimental arrangement the variable used to give an indication of film breakdown is the torque exerted on the slider by the

---

*Superscripts refer to numbered items in the bibliography.

circulation of the air between the plates. In addition, the mean film thickness and the amplitude of wobble are measured under all test conditions. Finally an indication of the rate of pressure buildup and decay is determined by measuring the response of the variables to a step and impulsive change in the load.

II. DESCRIPTION OF APPARATUS

2.1 Introduction

The experimental apparatus, shown in figure 2.1, consists of three major units:

1. The lower thrust plate supported in the center by a small diameter pin which acts as a flexure, allowing the plate to wobble around the edge while the center is held fixed.

2. The magnetic assembly which provides the excitation forces required to wobble the lower thrust plate. This magnetic assembly is shown in figure 2.2.

3. The upper thrust plate (shown in figure 2.3) which is supported in an air lubricated journal bearing.

In addition to these major components there is associated instrumentation used to measure:

1. Axial load.

2. Torque exerted on the upper plate by the circulating air film.

3. Current passing through each of the exciting magnet coils.

4. Mean film thickness (film thickness at the center of the plates).

5. Amplitude of the wobble.

The entire layout assembly is shown in figure D.1. Figure D.2 shows the entire experimental arrangement including the associated instrumentation.

Figure 2.1a Photograph of the bearing test apparatus

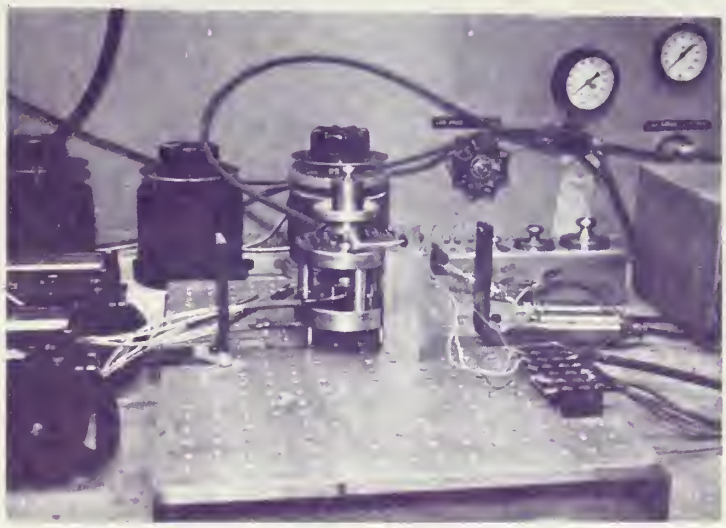

Figure 2.1b Photograph of experimental setup of test apparatus

Figure 2.1

Figure 2.2a Magnet Assembly

Figure 2.2b Lower thrust plate assembly

Figure 2.2

2.2 Lower Thrust Plate

The lower wobble plate is a disk 1-3/4" in diameter and 1/8" thick made of heat treated (56 RC) 440 stainless steel. It has a bearing surface 1-1/2" in diameter which is lapped flat to a finish of about 8 micro inches. The center of the plate is supported on a steel pin 3/32" in diameter. Acting as a cantilever, this pin allows the plate to tilt when a moment is applied to the end by any one of the magnets. By adjusting the position of the locknuts on this pin the air gap between the face of the magnets and the wobble plate may be varied. The air gap was kept constant at 0.006" throughout the entire experiment.

2.3 Magnet Assembly

Three magnets spaced at 120° intervals under the wobble plate constitute the magnet assembly. A brass plate is used to mount each of the magnets to the lower support plate. Each magnet has a laminated sheet steel core over which a nylon bobbin wound with 90 turns of No. 25 Formvar insulated copper wire is placed. The coils are energized by a three phase voltage source controlled by three separate Variacs, "wye" connected to the primary 208 volt power supply. To allow a fine adjustment of coil current a potentiometer was connected in series with each coil. Figure 2.2a shows the three magnets mounted on the lower support plate. The entire wobble assembly, including the lower thrust plate supported on its support pin, is shown in figure 2.2b. The electrical circuit is shown schematically in Appendix D.

2.4 Upper Thrust Plate

Figure 2.3 shows the upper thrust plate, consisting of a 1/8" thick disk integral with a 3/8" diameter shaft, of heat treated (56 RC) 440 stainless steel. The face of the disk is ground perpendicular to the shaft and lapped flat to a finish of about 8 micro inches. An air lubricated journal bearing* supports the shaft radially while allowing freedom of movement in the axial direction. The journal bearing is held in an upper support plate bolted to the lower support plate, the bolts passing through three spacers. The lengths of the spacers, shown in figure 2.1, are adjusted to insure that the upper and lower thrust plates are exactly parallel.

2.5 Instrumentation

In order to apply the axial load to the bearing, a small aluminium pan was clamped to the end of the shaft extending above the journal bearing. The bearing load was varied by placing standard laboratory weights in the pan. The actual load on the bearing was then simply the weight of the upper thrust assembly, 2.5 ounces, plus the applied standard weights. This arrangement can be seen in figure 2.1.

Also shown in figure 2.1 is the device which was used to measure the torque on the upper thrust plate. Clamped to the weight pan is a radial arm balanced between the pull of two tension springs, one pulling from each side of the arm. As torque is exerted on the shaft the springs

*For details of journal bearing construction see Appendix B.

Figure 2.3 Upper thrust plate with capacitor probes

deflect, allowing an iron slug, connected to the end of the radial arm by a brass rod, to move in or out of an LVDT depending upon the direction and magnitude of the torque. The input to the LVDT was supplied by an oscillator set at 0.5 KC and 6 volts. The output was rectified and measured with a vacuum tube DC voltmeter. Known torques were applied to the shaft in order to obtain a calibration curve which could be used to convert the voltage output of the LVDT directly to ounce-inches of torque*.

Three AC ammeters were connected in series with the magnetic coils to measure the exciting current directly. Each of the ammeters was set to read values of RMS current in the 0 to 2.5 ampere range.

Both the mean film thickness, measured at the center of the thrust plates, and the amplitude of the wobble, measured at the periphery, were measured indirectly by electrical means. A Decker 102-1 monitoring unit and two Delta probes were used for this purpose. Since the outputs of the Delta units vary with the difference between two connected capacitances, a reference capacitor of 15 mmf was connected across one set of terminals on each probe. The other set of terminals were connected to the grounded lower thrust plate and small round probes located in the upper thrust plate. The small probes in the upper plate and the grounded lower plate constituted parallel-plate capacitors with the film of air between the plates acting as a dielectric. With the probes connected as described above the output of the monitoring unit

*The calibration curve for the torque meter is included in Appendix C.

corresponded to a relative change in distance between the small probes and the lower plate, i.e. a change in capacitance. By measuring these electrical outputs on a dual-beam oscilloscope a time varying display of the film thickness at the center and periphery of the plates could be displayed*. At times during the experiment it was considered desirable to investigate the nature of the wobble. For this purpose a second probe 90^{o} away from the first was located on the periphery of the upper plate. By displaying the output of these two probes on the oscilloscope and measuring the phase difference between them the nature of the wobble was determined.

*The calibration procedure used and the resulting calibration curves are included in Appendix C.

III. OPERATION OF APPARATUS

The bearing assembly, associated instrumentation and wiring were set up as described in Section II and Appendix D. It was found that to obtain consistent results the two thrust plates had to be exactly parallel. To accomplish this, shim stock graduated in 0.0001" from 0.001" to 0.002" was placed below the spacers. To check the parallelism between the plates: 1. The regulated air supply to the journal bearing (190 psig) was turned on. 2. The Decker unit and oscilloscope were turned on. 3. The upper thrust assembly was slowly rotated 360° while the output of a capacitor probe, located on the edge of the plate, was observed on the scope. When the DC output was constant around the entire 360° of rotation the plates were exactly parallel.

To make a complete test run the following steps were taken:

1. The Decker unit, oscilloscope, oscillator and DC voltmeter were energized and a 2 minute warm-up period was allowed.

2. The air supply to the journal bearing was turned on and regulated to 190 psig.

3. The three phase power supply was turned on and the Variacs were adjusted to give about a 2 volt output.

4. The potentiometers were adjusted until the desired current was flowing in all the magnetic coils.

5. A weight was placed on the pan which was heavy enough to cause the two plates to come in contact with each other. The vertical

bias of each beam of the oscilloscope was set to a pre-selected zero.

6. The weight was removed and the readings of the DC voltmeter (torque), the ammeters and the mV output of the capacitor probes displayed on the oscilloscope (film thickness and amplitude of wobble) were recorded.

7. All the data for successive runs, with incremental increases in load, (addition of laboratory weights to the pan) were recorded.

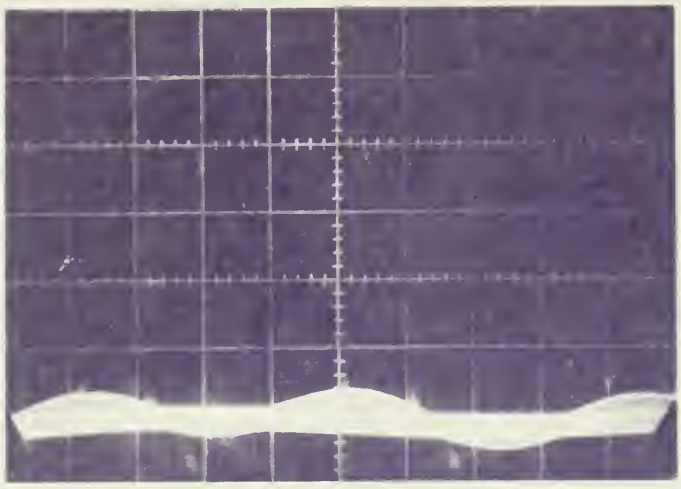

Figure 3.1 Oscilloscope display corresponding to step No. 5 (adjustment of vertical bias)

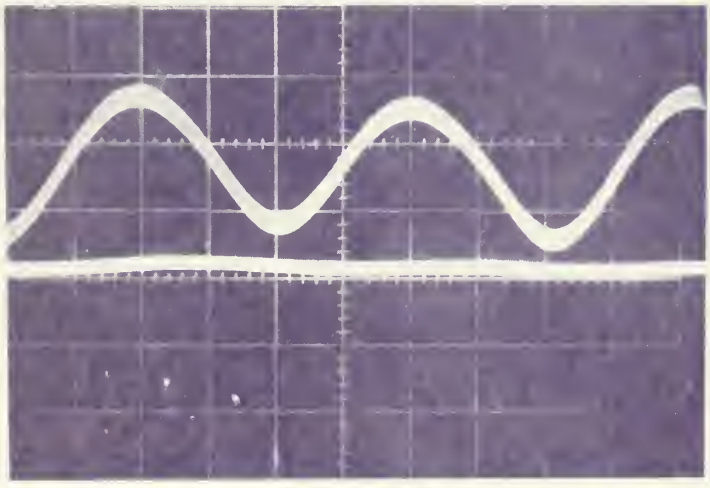

Figure 3.2 Oscilloscope display of bearing in operation. Lower trace is output of center probe and upper trace is output of a probe on the edge.

IV. PRESENTATION OF RESULTS

4.1 Discussion of Analytical Results

Nahavandi and Osterle[1] investigated a parallel-surface thrust bearing (figure 4.1) in which the slider was spinning and precessing with constant angular velocities Ω and ω respectively. The results of this experiment should correspond to their results for the case where Ω is set equal to zero, i.e. no rotation of the slider. Reynolds equation for a compressible lubricant is:

$$\frac{\partial}{\partial r}\left(\rho\, r\, h^3 \frac{\partial p}{\partial r}\right) + \frac{\partial}{\partial \theta}\left(\frac{\rho h^3}{r}\frac{\partial p}{\partial \theta}\right) = 6\mu r\,(\Omega - 2\omega)\frac{\partial}{\partial \theta}(\rho h) \qquad (1)$$

In Nahavandi and Osterle's analysis, constant air viscosity, and isothermal conditions, were assumed. The authors converted equation (1) to dimensionless form:

$$\frac{\partial}{\partial \bar{r}}\left(\bar{\rho}\,\bar{r}\,H^3 \frac{\partial \bar{p}}{\partial \bar{r}}\right) + \frac{\partial}{\partial \theta}\left(\frac{\bar{\rho} H^3}{\bar{r}}\frac{\partial \bar{p}}{\partial \theta}\right) = G\,\bar{r}\,\frac{\partial}{\partial \theta}(\bar{\rho} H) \qquad (2)$$

and expressed equation (2) in a finite difference form which was suitable for an iterative solution on a high speed digital computer. The solution of equation (2) gave the authors the pressure distribution corresponding to various combinations of radius ratio, k; attitude, n; and bearing number, G*. By numerical integration they obtained values of the load per unit area from the pressure distribution. The curves showing the

*See Appendix A for definition of G.

FIGURE 4.1

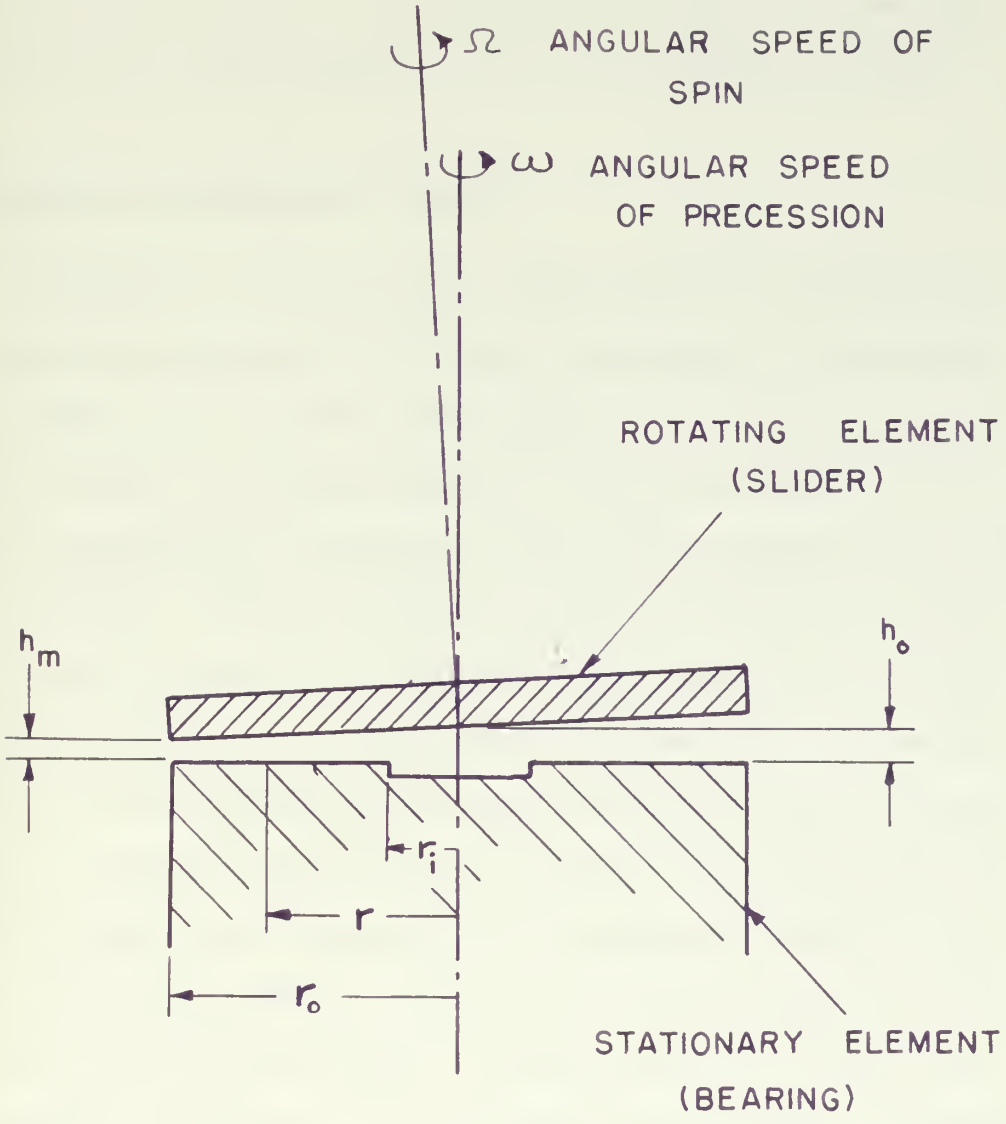

Parallel surface thrust bearing with a steady precession

relationship between load per unit area, P, k, n, and G are shown in figures 5a, b and c of reference 1.

Figure 4.2 is a plot of load W vs. attitude n, for the various values of bearing number G, corresponding to the geometry of the experimental thrust bearing. Both the analytical results of Nahavandi and Osterle and the experimental results of this study are plotted.

4.2 Discussion of Experimental Results

Data which was recorded during the operation of the test apparatus is tabulated in Appendix C and shown graphically on the following pages. Figure 4.3a is a plot of the torque exerted on the upper plate by the circulating air film and the axial load on the bearing. The apparent contradiction of decreasing torque with an increase in load is easily explained. When the bearing is operating as desired, the film of air between the plates is circulating with a maximum angular velocity close to ω. However, as the load is increased, the film becomes too thin for the circulation to be maintained and the torque increases rapidly with further increase in load. If the load is increased still further the torque will decrease until it reaches zero, when the two plates are in actual contact. It should be noted that when the bearing is operating in the desired range, the torque required to rotate the upper assembly is very low, i.e. less than 0.1 ounce-inches. The torque required to rotate the upper assembly for heavy loads is very high, although the measured torque is close to zero. In this second low torque region there is no air lubrication and the applied torque must overcome

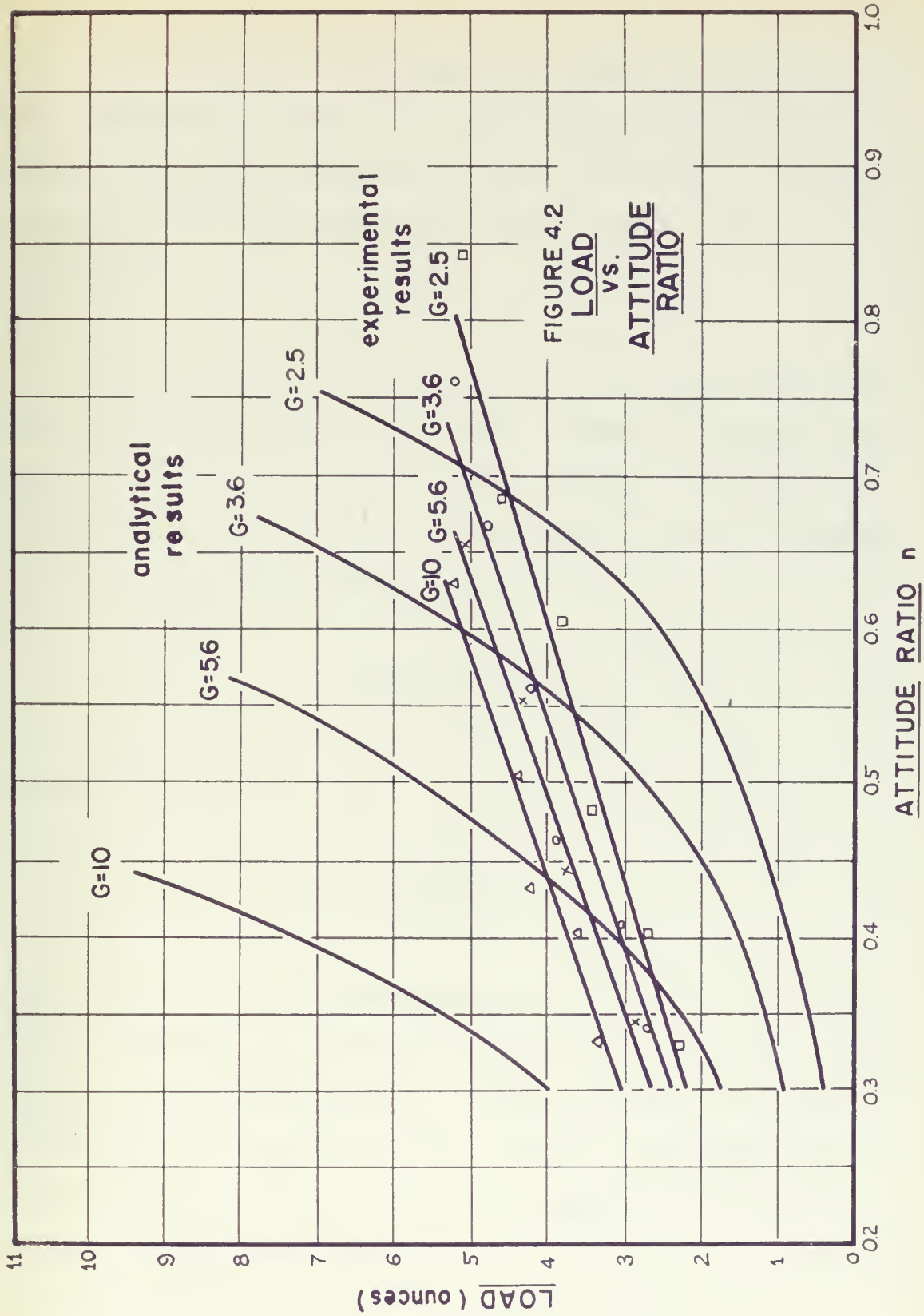

FIGURE 4.2
LOAD
vs.
ATTITUDE
RATIO

both static friction and surface adhesion between the plates. The results presented in figures 4.2, 4.3b, 4.4 and 4.5 are for the low torque region, where circulation of the air film occurs. A plot of torque vs. load for the region under investigation is shown in figure 4.3b.

The data required to plot the curves of attitude ratio n and load W, with bearing number G as a fixed parameter, is obtained from the curves in figures 4.4 and 4.5. First the lines representing constant values of bearing number G are plotted on the curve of clearance h_o vs. load W according to the equation:

$$G = \frac{6\mu r_o^2 (\Omega - 2\omega)}{h_o^2 p_o} \qquad (3)$$

Since $\Omega = 0$:

$$G = \frac{12\mu r_o^2 \omega}{h_o^2 p_o} \qquad (4)$$

These values are shown as horizontal lines in figure 4.4. The value of the load supported, at a particular setting of the magnetic coil current and a particular bearing number G, is simply the value of the load at the intersection of these two curves. For this same magnetic coil current and clearance h_o, the value of the amplitude of the wobble $h_o - h_m$ is obtained from figure 4.5, a plot of $h_o - h_m$ vs. h_o. From these values an attitude ratio n may be calculated according to:

$$n = \frac{h_o - h_m}{h_o} \qquad (5)$$

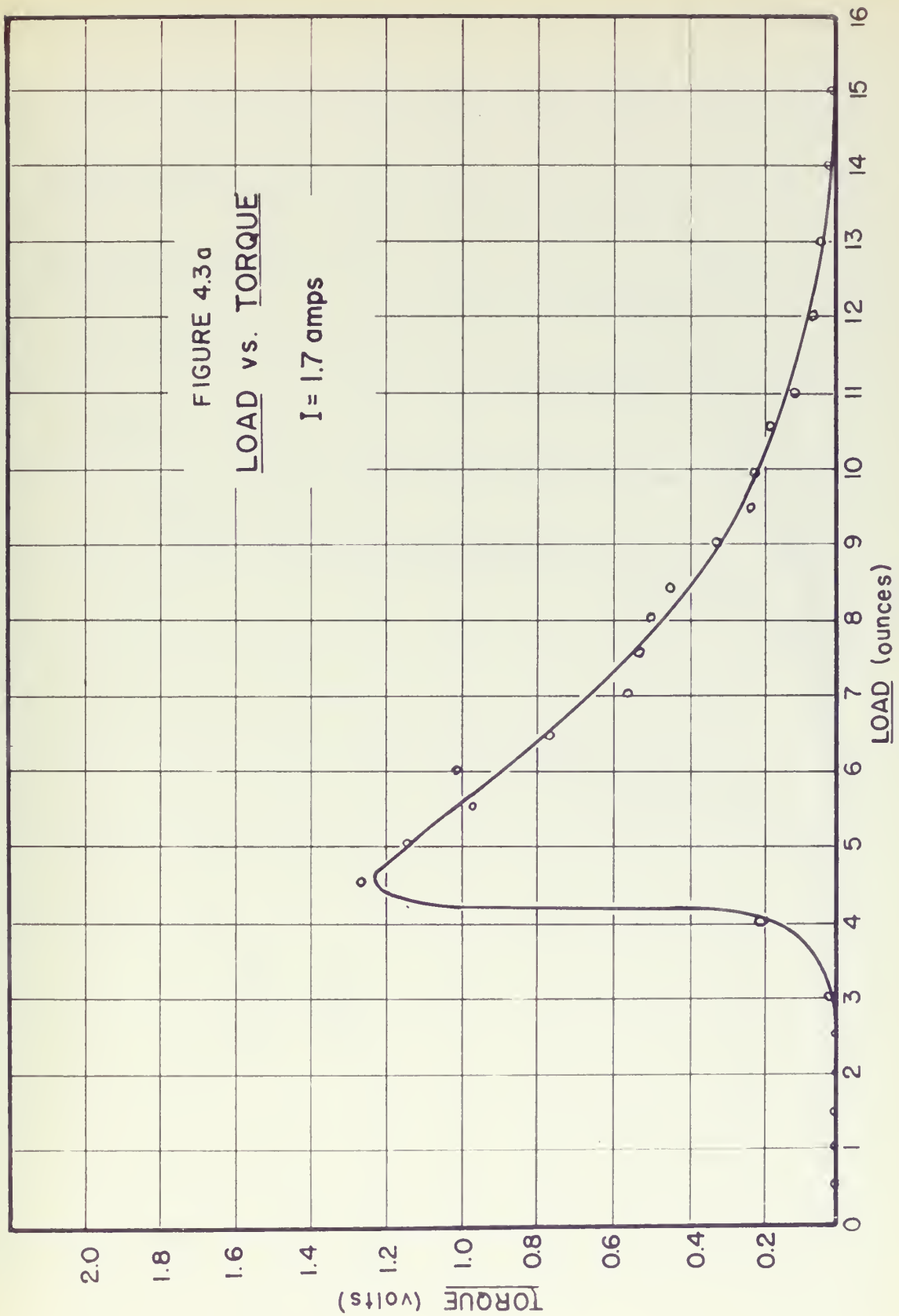
FIGURE 4.3a
LOAD vs. TORQUE
I = 1.7 amps
TORQUE (volts)
2.0
1.8
1.6
1.4
1.2
1.0
0.8
0.6
0.4
0.2
0
1
2
3
4
5
6
7
8
9
10
11
12
13
14
15
16
LOAD (ounces)

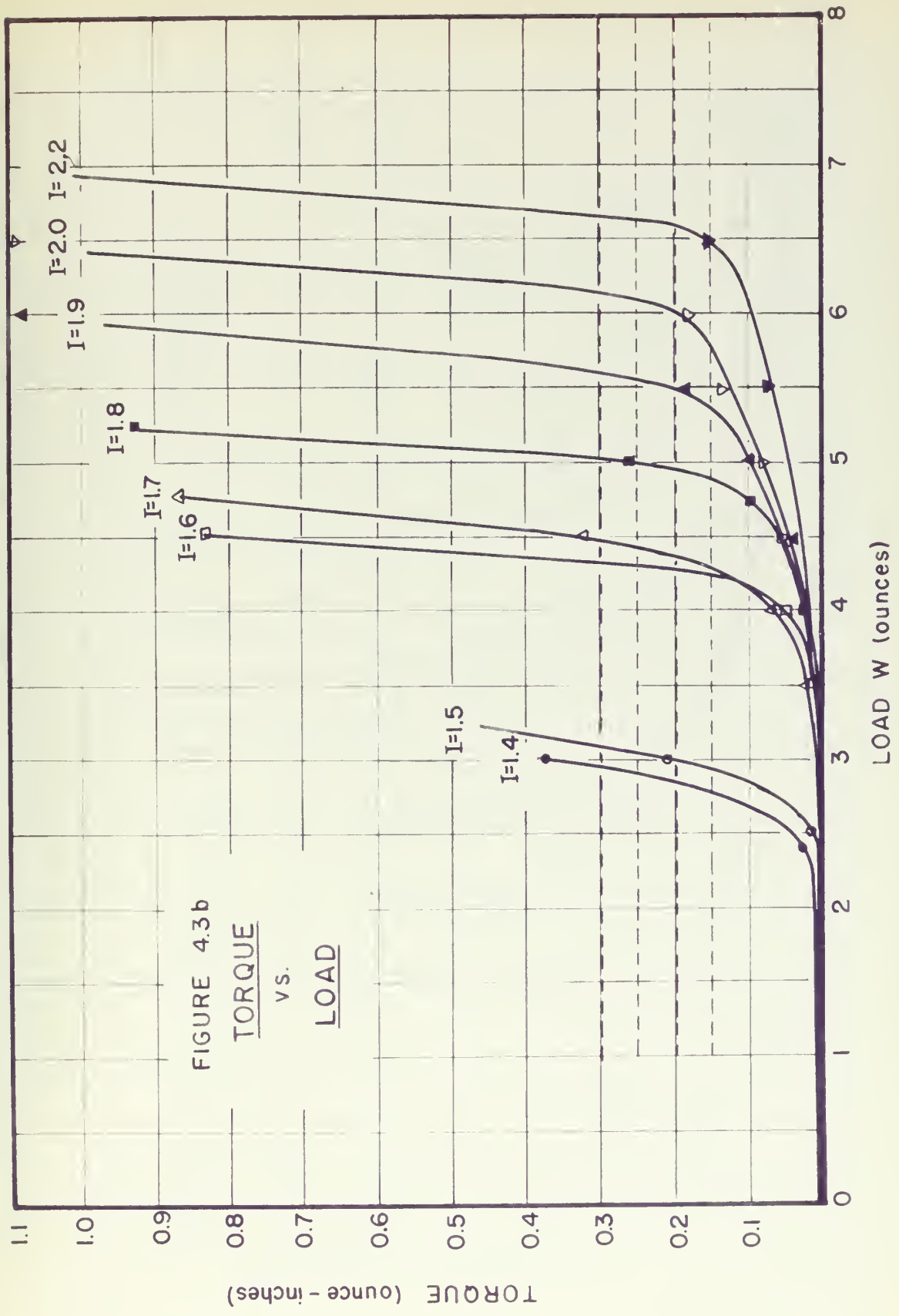

FIGURE 4.3b
TORQUE
vs.
LOAD

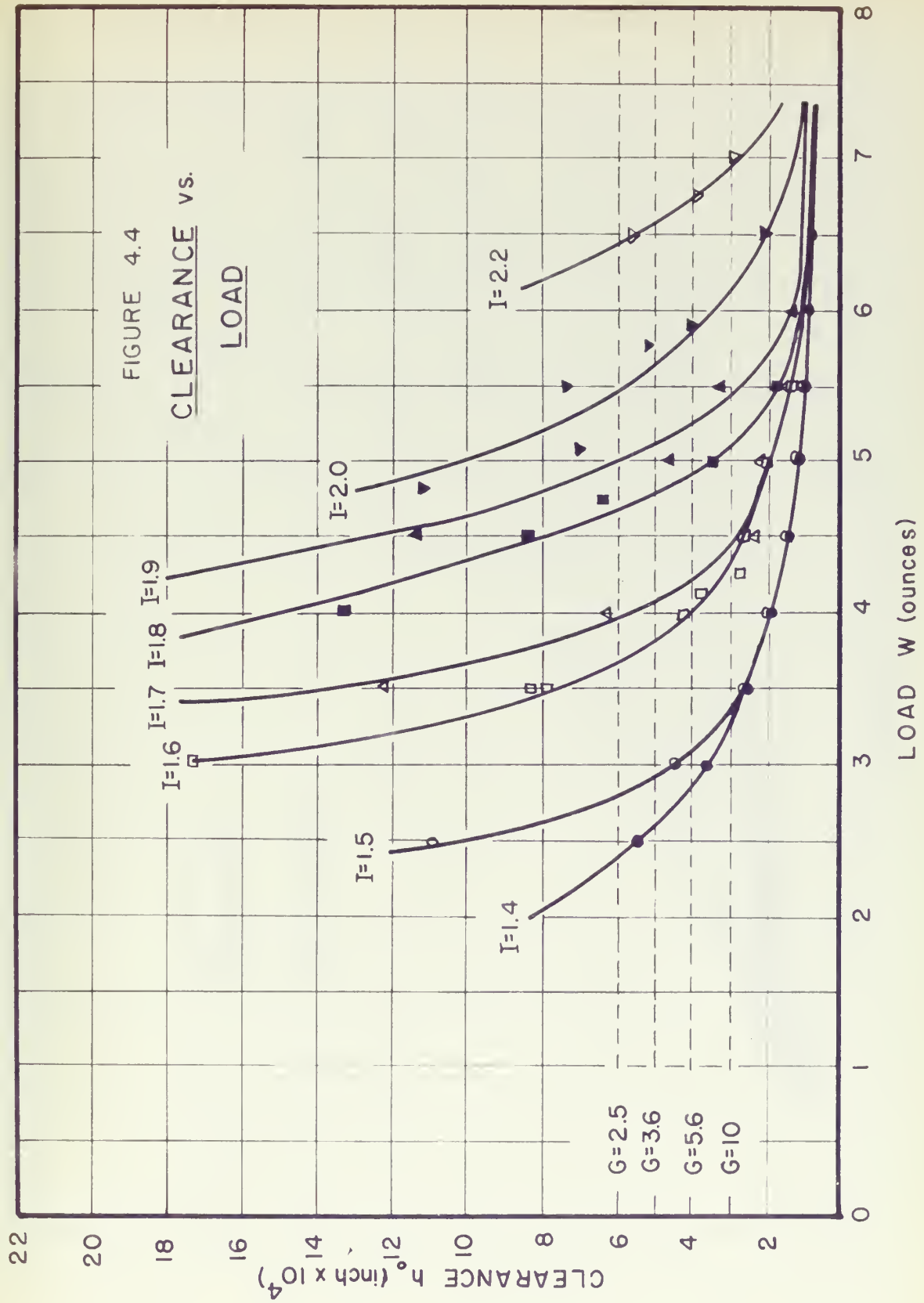
FIGURE 4.4
CLEARANCE vs.
LOAD
I=1.4
I=1.5
I=1.6
I=1.7
I=1.8
I=1.9
I=2.0
I=2.2
G=2.5
G=3.6
G=5.6
G=10
CLEARANCE h_o (inch x 10^4)
LOAD W (ounces)
0
1
2
3
4
5
6
7
8
2
4
6
8
10
12
14
16
18
20
22

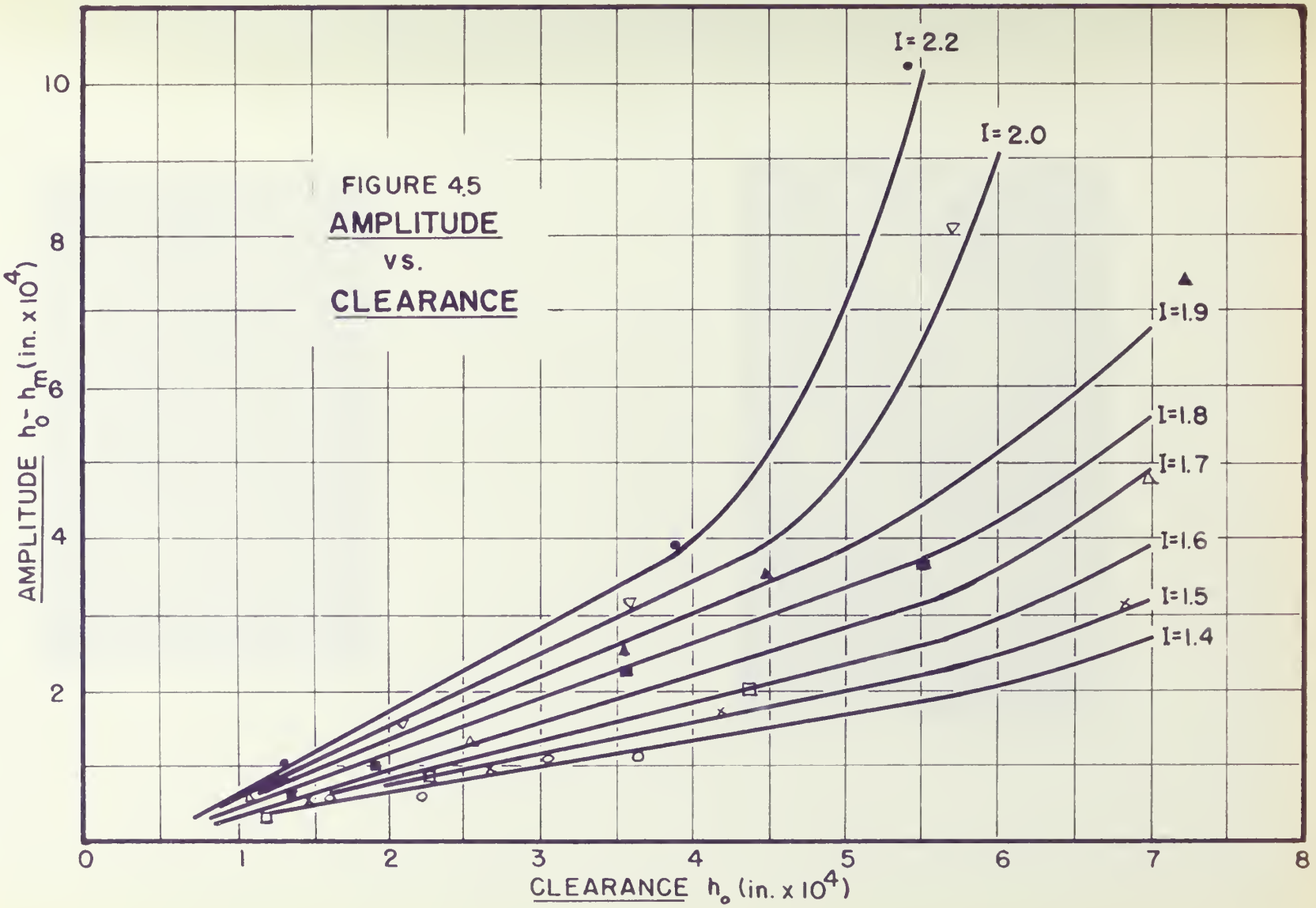
FIGURE 4.5
AMPLITUDE
VS.
CLEARANCE
I= 2.2
I= 2.0
I=1.9
I=1.8
I=1.7
I=1.6
I=1.5
I=1.4
AMPLITUDE $h_o - h_m$ (in. x 10^4)
CLEARANCE h_o (in. x 10^4)
0
1
2
3
4
5
6
7
8
2
4
6
8
10

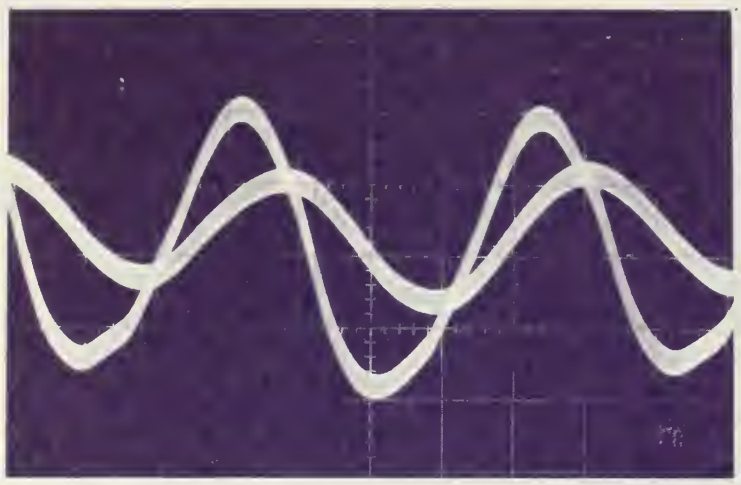

Figure 4.6 Oscilloscope display of two outer capacitor probes. Note 90^{o} phase difference (50 mV/cm, 2 x 10^{-3} sec/cm)

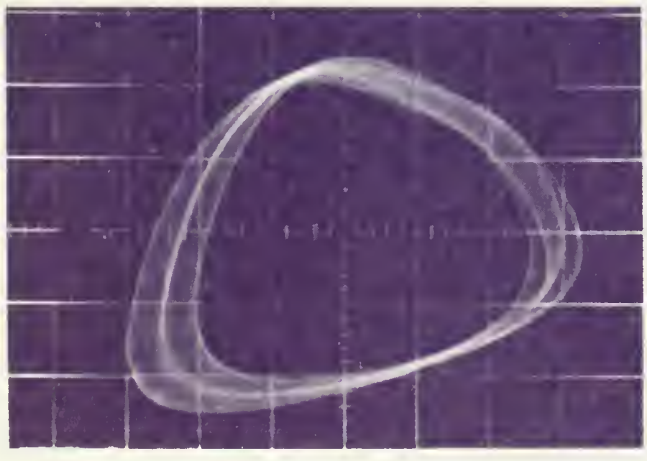

Figure 4.7 Lissajous pattern showing 90^{o} phase difference between output of two capacitor probes.

Numerical Example:

From figure 4.4 and equation (4):

magnetic coil current	1.7 amps
clearance h_o	0.0005"
$G = \frac{12\mu r_o^2 \omega}{(.0005)p_o}$	3.6
load W	4.10 ounces

From figure 4.5 and equation (5):

amplitude $h_o - h_m$	0.00028"
$n = \frac{h_o - h_m}{h_o}$	0.56

From figure 5c[1]:

radius ratio k	0.25
load per unit area P	0.14 psi
$W = 16\pi (0.75)^2 p$	3.94 ounces

The phase difference between the outputs of the two capacitor probes, located on the periphery of the upper plate, was 90° for all operating conditions. This indicates that the motion of the lower plate was a true precessional wobble. The wobble frequency also remained constant, at 120 cps, for all conditions of operation. Figures 4.6 and 4.7 show the outputs of the two outer probes displayed on the dual beam oscilloscope. To obtain the display shown in figure 4.6, both outputs were connected to the vertical input plates. The display in figure 4.7 was obtained by connecting one output to the vertical input and the other

to the horizontal input of the oscilloscope. This second display is the Lissajous pattern corresponding to a phase difference of 90°, i.e. a circle.

From the slope of the curves in figure 4.4 an average value of the bearing stiffness k_o may be obtained, e.g. 2500 ounces per inch when the mean film thickness h_o is 0.0005". A comparison of figures 4.3b and 4.4 shows that the circulation of the air film breaks down when the mean air film thickness reaches a value of about 0.00045".

The responses of the bearing to a step change in load and a random impulse are shown in figures 4.8 and 4.9 respectively. A study of these oscilloscope displays shows that the time response for decay of the film thickness, 0.3 seconds, is about the same as the time required for pressure buildup. The undamped, natural frequency of the unloaded, upper plate assembly, calculated from k_o and the 2.5 ounce mass is 98 cps.

4.3 Comparison of Results

Both the results of this study and the results expected from Nahavandi and Osterle's analysis are shown in figure 4.2*, a plot of W vs. n with bearing number G as a fixed parameter. Although agreement between experimental and analytical results is poor, the increase in load capacity with an increase in either bearing number or attitude ratio is as expected. The experimental results show a linear increase in W with

*Tabulated values are in Appendix C.

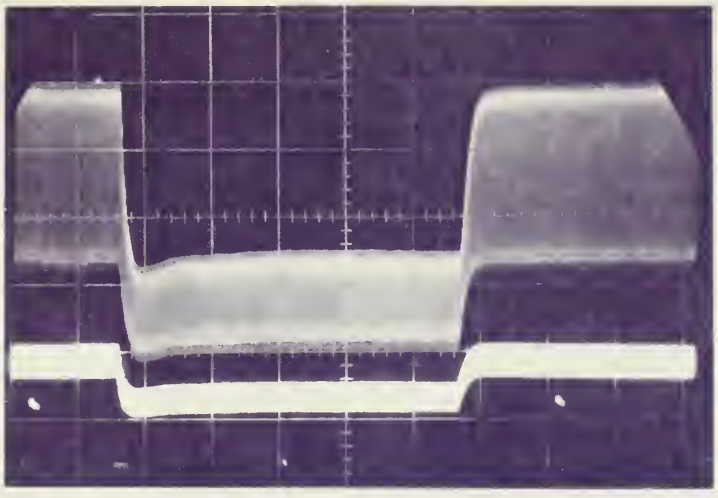

Figure 4.8 Response to a unit step change in load. (1 sec/cm, 50 mV/cm)

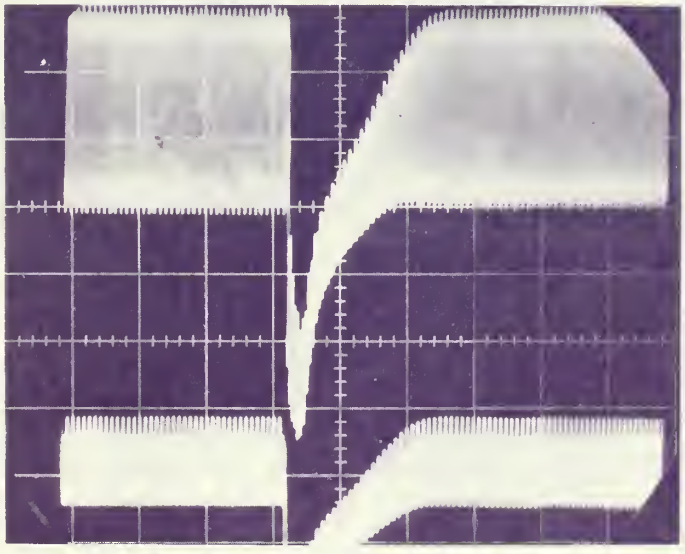

Figure 4.9 Response to a random impulse in load. (0.2 sec/cm, 50 mV/cm)

an increase in n, whereas, the analytical results predict an almost square law increase in W. A possible reason for the poor agreement is that, in the experiment, the lower plate began to bend slightly when the magnetic coil currents were increased to the higher values. The result of this bending was an increase in the attitude ratio causing the load curve to flatten out.

4.4 Possible Applications

The magnetically-excited, self-acting, gas lubricated thrust bearing investigated in this thesis can be used where design requirements are such that there is no pressurized gas supply available and the relative movement between the slider and the bearing is close to zero, such as in a rate gyro. These design requirements preclude the use of either pressurized hydrostatic bearings or self-acting, hydrodynamic, gas lubricated bearings, such as tilting pad bearings, step bearings, bevel bearings or fixed tapered land bearings. The only requirement for this bearing is the need of a 3 phase power supply of about 3 - 6 watts.

APPENDIX A

Nomenclature

B_m magnetic flux density

d orifice diameter

D diameter of shaft

F magnetic force

F_o journal bearing number for 6 orifice holes $\sqrt{\frac{k-1}{2kRT_s g}} \frac{P_s D h_r^2}{4.6\mu 0.9 L d}$

G thrust bearing number $\frac{6\mu r_o^2 (\Omega - 2\omega)}{h_o^2 p_o}$

h_o mean film thickness at the center of the plate

h_m minimum film thickness

h_r radial clearance

H dimensionless film thickness $\frac{h}{h_o}$

I magnetic coil current

k radius ratio $\frac{r_i}{r_o}$

k_o bearing stiffness

L length of journal bearing

n attitude ratio $\frac{h_o - h_m}{h_o}$

N number of turns on magnetic coils

P load per unit area $\frac{W}{\pi r_o^2}$

p_o atmospheric pressure

r_i inside radius

r_o	outside radius
$\bar{r}$	dimensionless radius ratio $\frac{r}{r_o}$
R	gas constant
T_s	supply temperature
W	load capacity
λ	slider angle of tilt
μ	gas viscosity
ρ	gas density
ω	angular velocity of precession of disk axis
Ω	angular velocity of spin around disk axis

APPENDIX B

B.1 Wobble Assembly

Mounting the lower thrust plate on three piezoelectric crystals was first considered as a possible means of driving the wobble plate. However, the voltage required to deflect the crystal the necessary amount would be much too high to be practical.

Example:

Consider a 1" long barium titanate crystal with a piezoelectric constant = 155×10^{-12}. For a total elongation of 0.0002" the strain is:

$$\frac{\Delta \ell}{\ell} = \frac{0.0002}{1} = 2 \times 10^{-4} \text{ inches}$$

Since:

$$\frac{\Delta \ell}{\ell} = d_{33} E_3$$

$$E_3 = 1.29 \times 10^{4} \frac{\text{VOLTS}}{\text{CM}}$$

where:

E_3 = field strength

d_{33} = piezoelectric constant.

The required voltage to elongate the crystal 0.0002" is therefore 4.4×10^{7} volts, much too high to be practical in this application.

Use of magnetostrictive crystals was eliminated for the same reason.

It was then decided to mount the plate on a center flexure with three small electromagnets providing the necessary driving forces to wobble the plate (see figure D.1). The magnet cores were taken from three transistor output transformers and mounted, 120° apart, on the lower support plate, with the center poles acting at a radius of 5/8". The moment acting on the plate with the magnets in this position and excited by a three phase voltage source is:

$$M = 0.916\ F \qquad (1)$$

where F is the force acting across the air gap at the center pole.

After deciding to make the support flexure 9/16" long and 3/32" in diameter, the force F required to tilt the plate the desired amount (0.0004" wobble amplitude) was calculated as follows:

Let:

λ = angle of tilt in radians

x = wobble amplitude

ℓ = length of support flexure

$E = 30 \times 10^6$ psi for steel

$x = r_o \lambda$ where $r_o = 0.750"$

$\lambda = 5.32 \times 10^{-4}$ radians

The equation for the angular deflection of the end of a cantilever beam is:

$$\lambda = \frac{M\ell}{EI} \qquad (2)$$

Substituting in equation (2) and solving for F:

$$F = 0.152 \text{ pounds.}$$

From the equation

$$B_m = \sqrt{\frac{2\mu_o F}{A}}$$

the required flux density was calculated to be

$$B_m = 890 \text{ gauss}$$

The equation relating ampere-turns to flux density and air gap length is:

$$NI = B_m \ell_o \qquad (3)$$

By substituting in equation (3) the required number of ampere-turns was found to be:

$$NI = 22.5 \text{ ampere-turns}$$

Since there are three air gaps in the magnetic circuit, the total number of ampere turns required in the coil is:

$$NI = 3 \times 22.5 = 67.5 \text{ ampere-turns}$$

This indicates that, with 90 turns of wire on each coil, the required current will be about 1.3 amperes.

B.2 Capacitor Probes

The capacitor probes are designed so that the capacitance associated with an air gap of 0.0002" is 10 mmf. The output of the Delta probes and Decker unit is linear around this value of capacitance. The capacitance of two steel plates separated by a film of air is:

$$C_o = 0.225 \frac{A}{h} \qquad (4))$$

where:

C_o = mmf

A = $inch^2$

h = inch.

By solving equation (4) for the area:

$$A = 8.9 \times 10^{-3} \text{ inch}^2$$

From the area, the diameter is calculated to be:

$$d = 2\sqrt{\frac{A}{\pi}} = 0.106"$$

B.3 Journal Bearing

The design of the journal bearing is shown in figure B.1. The bearing actually consists of two journal bearings, each with six supply orifices and an L/D ratio = 1, i.e. the length and diameter of the bearings are both 3/8".

In order to determine the diameter of the supply orifices the dimensionless bearing number F_o was set equal to 1.

$$F_o = \sqrt{\frac{k-1}{2kRT_s g}} \quad \frac{P_s D h_r^2}{48\mu\, 0.9 L d} = 1 \tag{5}$$

Solving equation (5) for d:

$$d = \sqrt{\frac{k-1}{2kRT_s g}} \quad \frac{P_s D h_r^2}{48\mu\, 0.9 L} \tag{6}$$

and substituting:

$R = 53.30 \ \frac{ft\text{-}lb}{lb\text{-}R^o}$ $\qquad$ $g = 32.2 \ \frac{ft}{sec^2}$

$D = 0.375" = 3.12 \times 10^{-2}$ ft $\qquad$ $k = 1.40$

$T_s = 530^o R$ $\qquad$ $P_s = 195$ psia $= 2.81 \times 10^4 \ \frac{lb}{ft^2}$

$h_r = 5 \times 10^{-4}$ in $= 4.16 \times 10^{-5}$ ft $\qquad$ $L = 3.12 \times 10^{-2}$ ft

$h_r^2 = 1.91 \times 10^{-9} \ ft^2$ $\qquad$ $\mu = 4.18 \times 10^{-7} \ \frac{lb\text{-}sec}{ft^2}$

the resulting orifice diameter is:

$$d = 1.17 \times 10^{-3} \text{ ft.} = 0.014"$$

A No. 80 drill is the closest standard drill size (0.0135").

FIGURE B.1

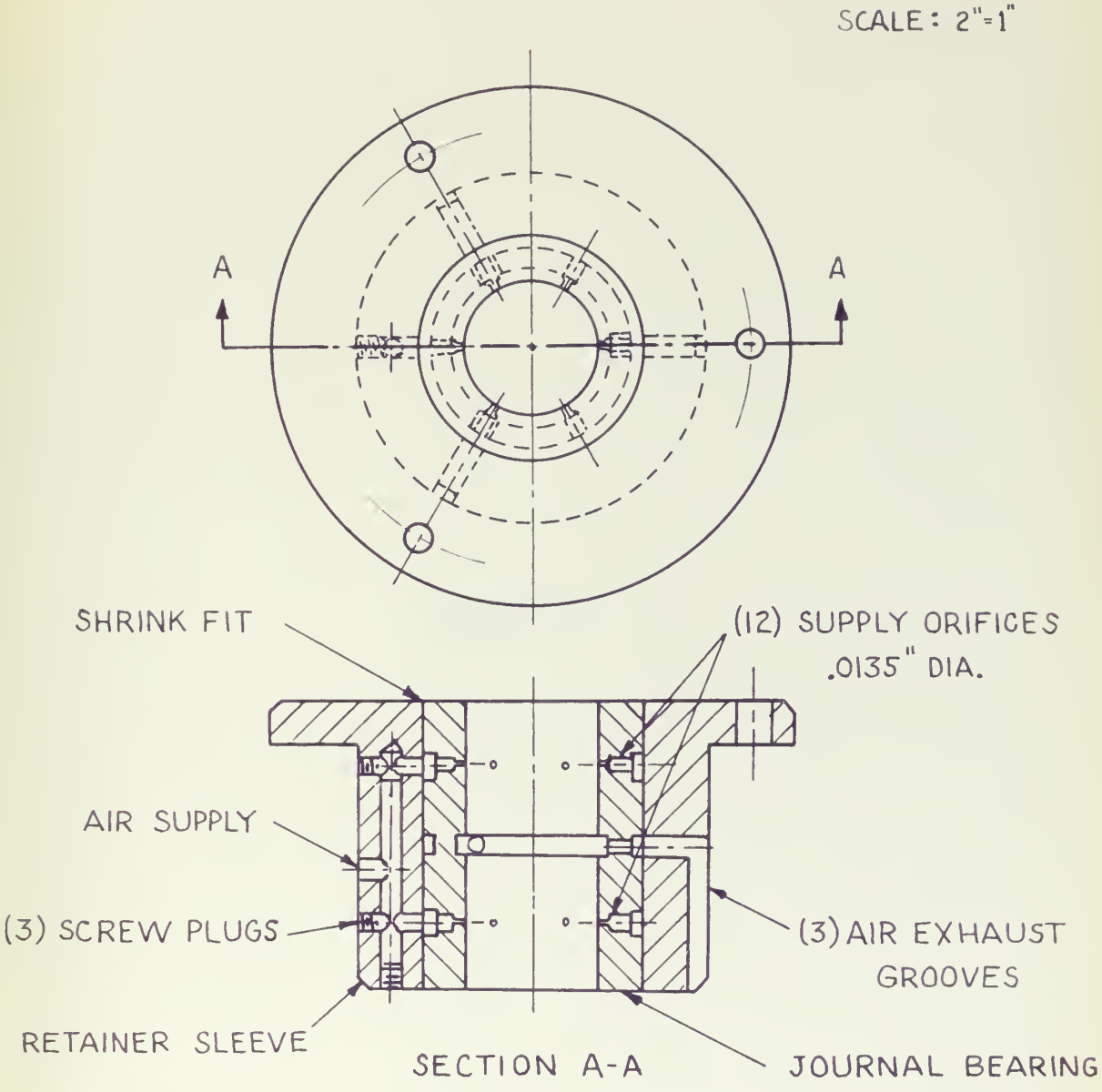

AIR- LUBRICATED
JOURNAL BEARING

APPENDIX C

TABLE C.1

EXPERIMENTAL RESULTS

I (amps)	W (ounces)	TORQUE (oz-in)	h_o ($in \times 10^4$)	$h_o - h_m$ ($in \times 10^4$)
1.4	2.5	0.03	5.5	1.9
1.4	3.0	0.38	3.6	1.2
1.4	3.5	-	2.3	0.8
1.5	2.5	0.00	11.0	6.9
1.5	3.0	0.42	4.3	1.7
1.5	3.5	-	2.6	1.0
1.6	2.5	0.00	20+	12.6
1.6	3.0	0.00	20+	9.0
1.6	3.5	0.01	8.0	7.6
1.6	3.5	0.01	8.4	8.0
1.6	4.0	0.04	4.4	1.9
1.6	4.0	0.05	4.4	1.8
1.6	4.25	0.13	4.0	1.7
1.6	4.5	0.18	2.3	0.8
1.7	2.5	0.00	20+	13.4
1.7	3.0	0.01	20+	12.6
1.7	3.5	0.03	12.0	11.2
1.7	4.0	0.07	6.8	4.8
1.7	4.5	0.88	2.5	1.4
1.8	2.5	0.00	20+	15+
1.8	3.0	0.00	20+	15+
1.8	3.5	0.00	20+	15+
1.8	4.0	0.02	12.6	12.0
1.8	4.5	0.05	8.4	7.4
1.8	4.75	0.10	5.4	3.6
1.8	4.75	0.11	4.6	3.1
1.8	5.0	0.18	3.7	2.4
1.8	5.0	0.17	4.0	2.7
1.8	5.25	1.00	1.8	1.0
1.9	2.5	0.03	20+	15+
1.9	3.0	0.01	20+	15+
1.9	3.5	0.01	20+	15+
1.9	4.0	0.05	20+	13.4
1.9	4.5	0.06	11.0	10.9
1.9	5.0	0.10	4.4	3.6
1.9	5.5	0.19	3.6	2.5
1.9	6.0	1.12	1.4	0.8
2.0	3.5	0.03	20+	15+
2.0	4.0	0.03	20+	15+
2.0	4.5	0.07	11.0	15+
2.0	5.0	0.10	5.7	8.1
2.0	5.5	0.15	6.6	11.4

TABLE C.1 (continued)

I	W	TORQUE	h_o	$h_o - h_m$
2.0	5.75	0.18	5.6	9.8
2.0	6.0	0.18	4.4	3.6
2.0	6.5	1.15	2.2	1.6
2.2	6.5	0.15	5.4	10.2
2.2	6.75	0.20	3.9	3.9
2.2	6.875	1.23	3.1	2.7

TABLE C.2

COMPARISON OF RESULTS

EXPERIMENTAL						ANALYTICAL	
h_o ($in \times 10^4$)	C	$h_o - h_m$ ($in \times 10^4$)	I (amps)	n	W (ounces)	P (load/unit area)	W (ounces)
4	5.6	1.4	1.4	0.350	2.8	0.08	2.25
4	5.6	1.6	1.5	0.40	3.1	0.11	3.10
4	5.6	1.8	1.6	0.45	4.0	0.16	4.50
4	5.6	2.2	1.7	0.55	4.2	0.26	7.33
4	5.6	2.6	1.8	0.65	4.9	0.44	12.40
4	5.6	3.0	1.9	0.75	5.3	0.71	20.00
4	5.6	3.4	2.0	0.85	5.8	1.30	36.80
4	5.6	3.9	2.2	0.97	6.8	2.20	62.20
5	3.6	1.7	1.4	0.34	2.6	0.04	1.13
5	3.6	2.0	1.5	0.40	2.9	0.05	1.41
5	3.6	2.3	1.6	0.46	3.8	0.08	2.25
5	3.6	2.8	1.7	0.56	4.1	0.14	3.94
5	3.6	3.3	1.8	0.66	4.8	0.26	7.33
5	3.6	3.8	1.9	0.76	5.1	0.43	12.10
5	3.6	4.9	2.0	-	-	-	-
5	3.6	7.2	2.2	-	-	-	-
6	2.5	2.0	1.4	0.33	2.3	0.017	0.48
6	2.5	2.4	1.5	0.40	2.7	0.026	0.73
6	2.5	2.9	1.6	0.48	3.6	0.045	1.27
6	2.5	3.6	1.7	0.60	3.9	0.088	2.48
6	2.5	4.1	1.8	0.69	4.6	0.16	4.50
6	2.5	5.1	1.9	0.85	5.0	0.44	12.40
6	2.5	-	2.0	-	-	-	-
6	2.5	-	2.2	-	-	-	-

TABLE C.2 (continued)

h_o	G	$h_o - h_m$	I	n	W	P	W
3	10	1.0	1.4	0.33	3.3	0.17	4.80
3	10	1.2	1.5	0.40	3.4	0.26	7.30
3	10	1.3	1.6	0.43	4.3	0.34	9.08
3	10	1.5	1.7	0.50	4.4	0.45	12.70
3	10	1.9	1.8	0.63	5.1	0.86	24.20
3	10	2.2	1.9	0.73	5.4	-	-
3	10	2.4	2.0	0.80	6.2	-	-
3	10	2.8	2.2	0.93	7.0	-	-

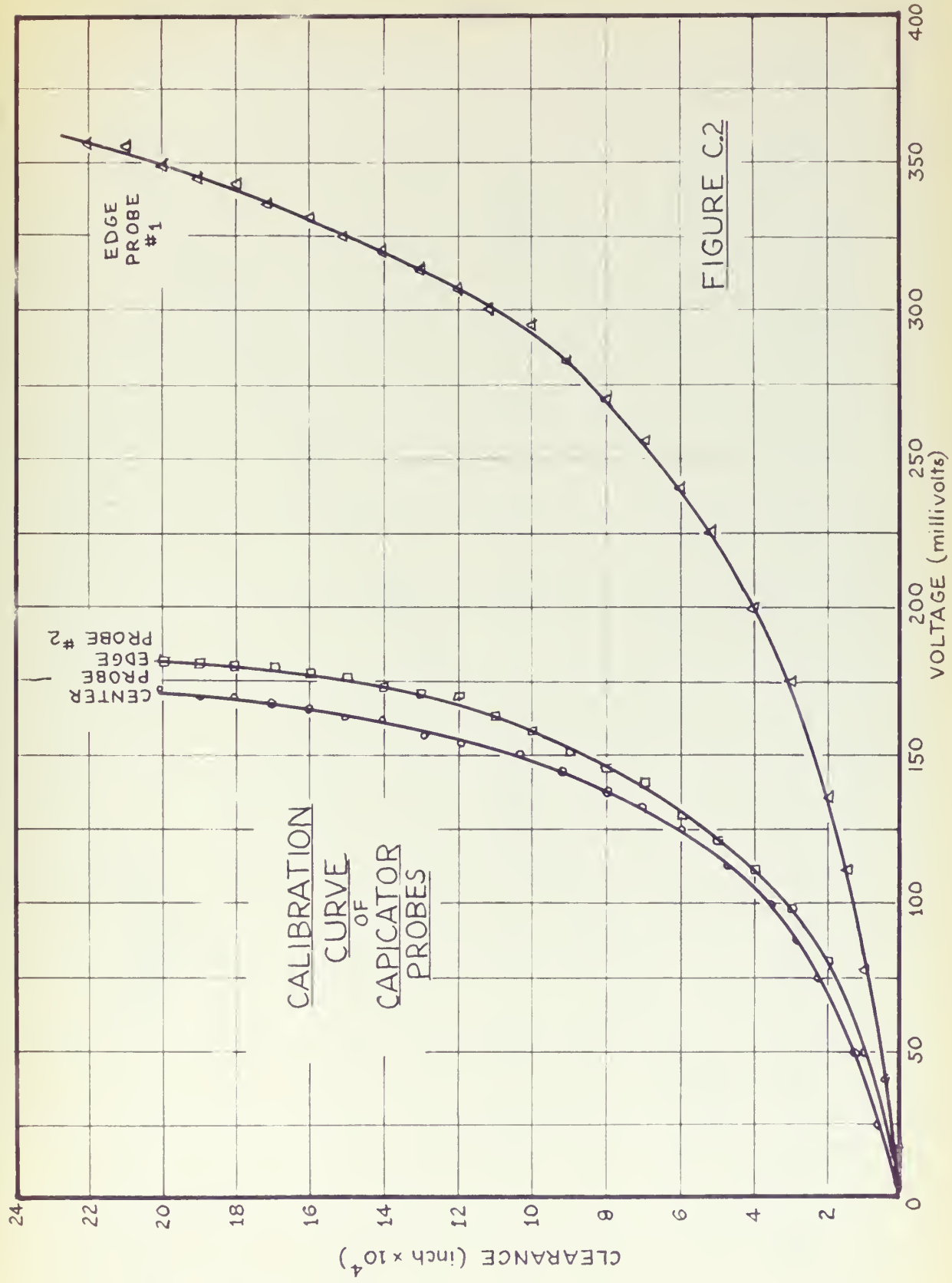
CALIBRATION CURVE OF CAPICATOR PROBES
EDGE PROBE #1
CENTER PROBE
EDGE PROBE #2
CLEARANCE (inch × 10⁴)
VOLTAGE (millivolts)
0
2
4
6
8
10
12
14
16
18
20
22
24
50
100
150
200
250
300
350
400

FIGURE C.2

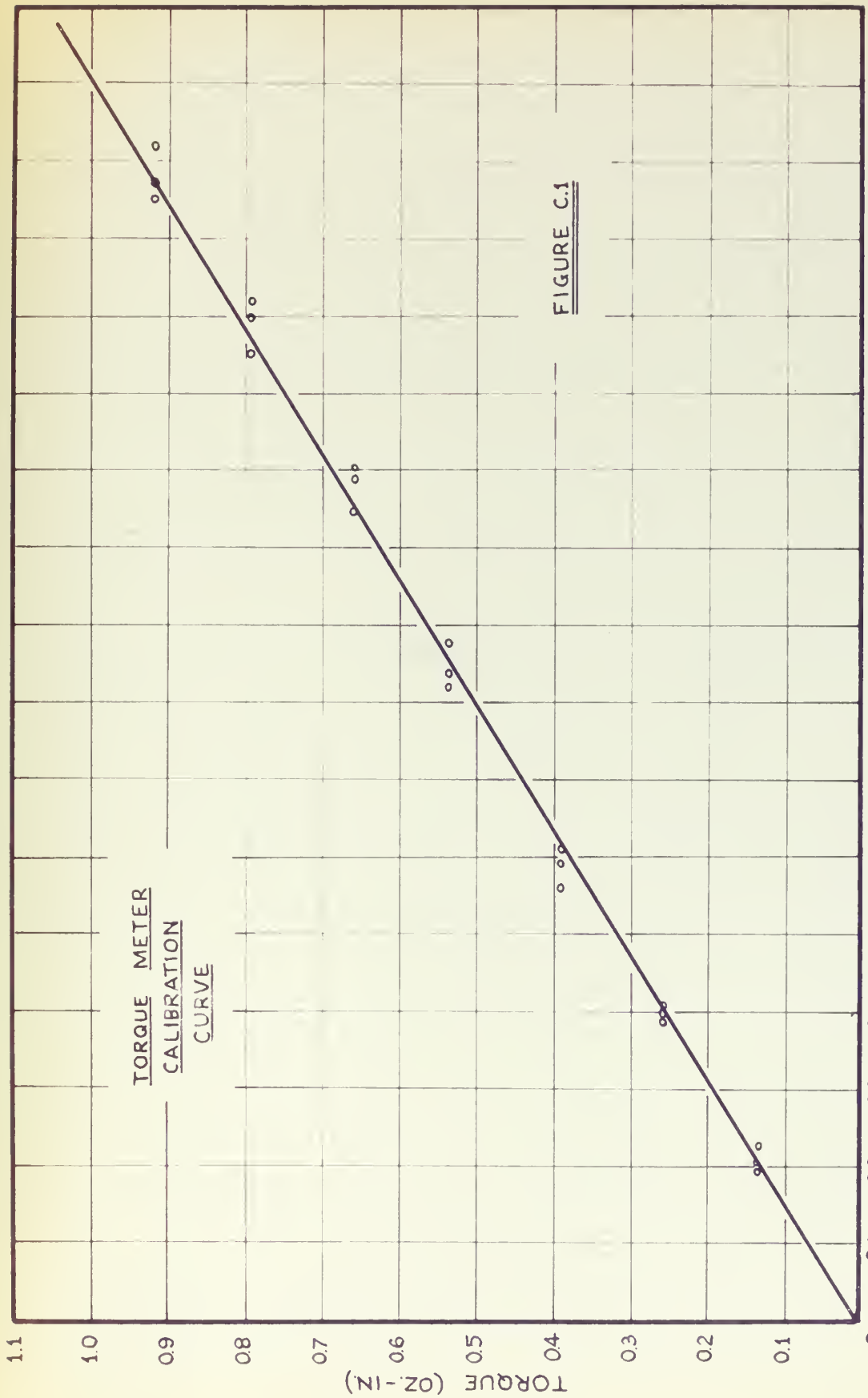
TORQUE METER
CALIBRATION
CURVE
TORQUE (OZ.-IN.)
LVDT OUTPUT (VOLTS)
0
0.1
0.2
0.3
0.4
0.5
0.6
0.7
0.8
0.9
1.0
1.1
1.2
1.3
1.4
1.5
1.6
1.7

FIGURE C.1

APPENDIX D

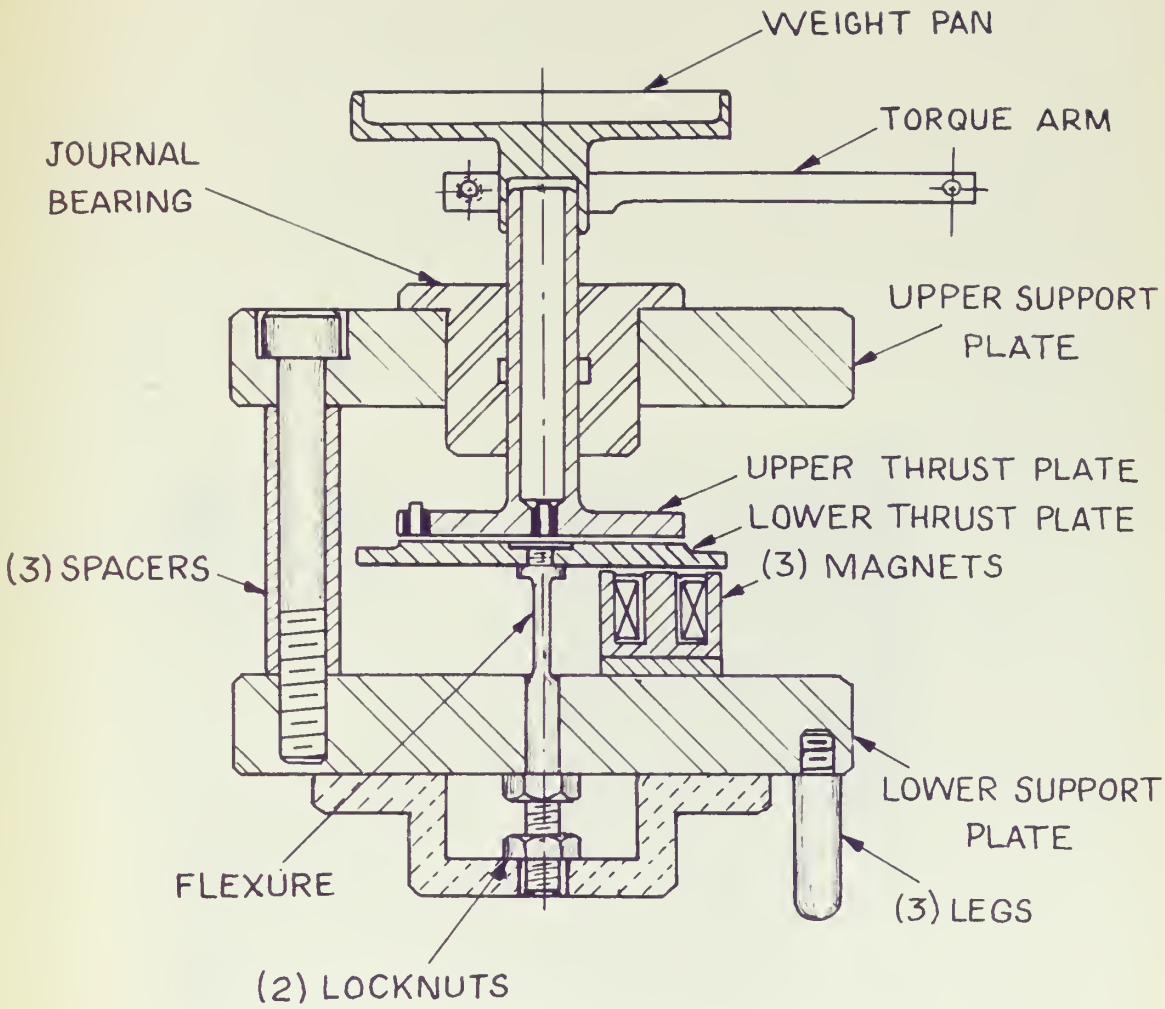

FIGURE D.1

TEST APPARATUS

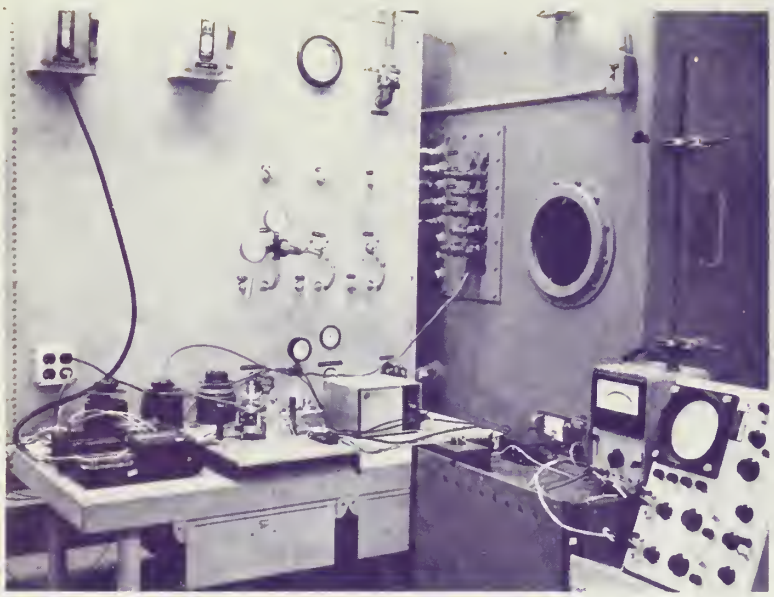

Figure D.2

Entire Experimental Setup

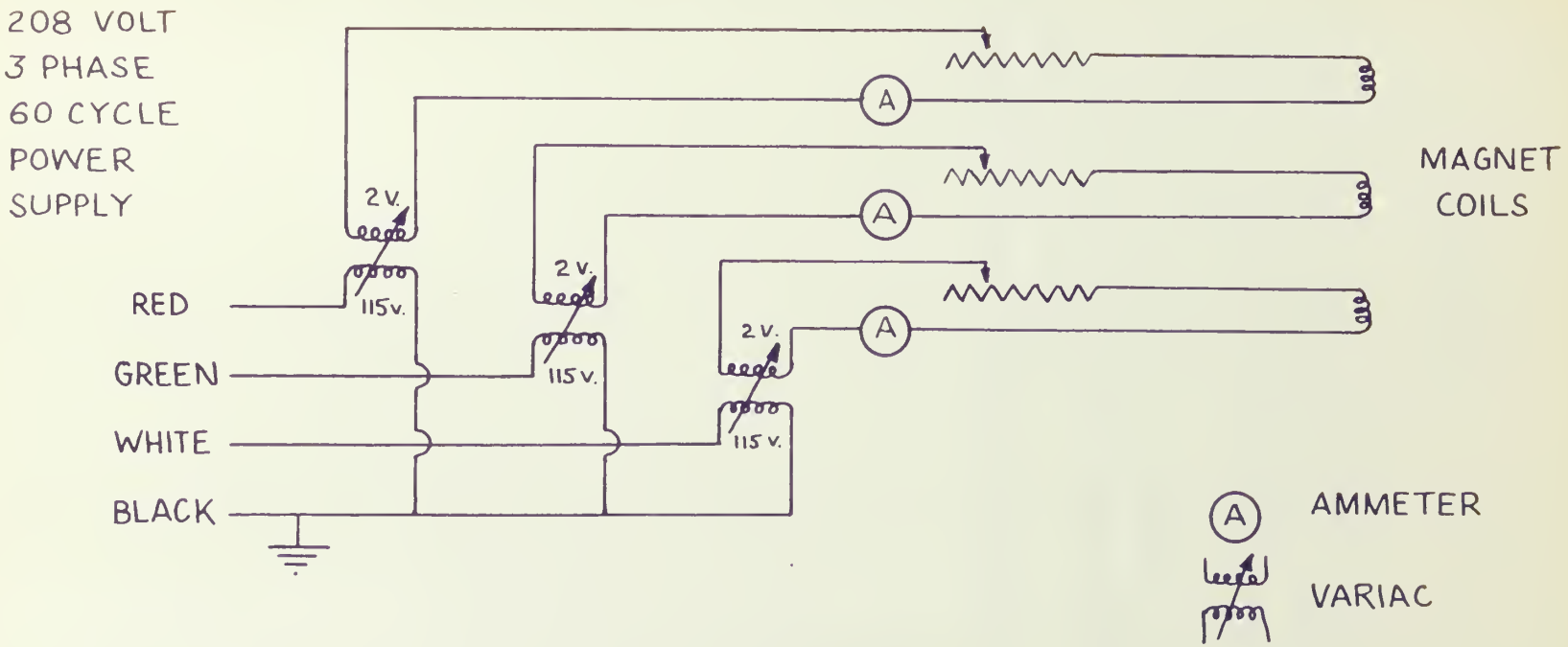

MAGNET EXCITING CIRCUIT

FIGURE D.3

BIBLIOGRAPHY

1. Nahavandi and Osterle, "A Novel Form of Self-Acting Gas Lubricated Thrust Bearing", ASLE Transaction 4, 124 - 130 (1961).

2. Fuller, "Theory and Practice of Lubrication for Engineers", John Wiley and Sons, Inc., New York.

3. Underhill, "Magnets", McGraw-Hill Book Company, Inc., New York.

4. Knowlton, "Standard Handbook for Electrical Engineers", McGraw-Hill Book Company, Inc., New York.

5. Marks, "Mechanical Engineers Handbook", McGraw-Hill Book Company, Inc., New York.